ELECTRICAL CONDUCTIVITY OF γ-Bi₂O₃–V₂O₅ SOLID SOLUTION

O. Turkoglu[1*] *and I. Belenli*[2]

[1]Department of Chemistry, Faculty of Art and Science, Erciyes University, 38039 Kayseri, Turkey
[2]Department of Physics, Faculty of Art and Science, Erciyes University, 38039 Kayseri, Turkey

Abstract

The total conductivity (σ_T) in *bcc* γ-Bi₂O₃ doped with V₂O₅ system has been measured in the composition range between 1 and 7 mol% V₂O₅ at different temperatures. Phase transitions for different addition amounts depending on the temperature were investigated by quenching the samples. According to the XRD and DTA/TG results, this *bcc* type solid solution was stable up to about 720°C and the solubility limit was found at ~7 mol% V₂O₅ in γ-phase. This system showed predominantly an oxide ionic conduction. As the V₂O₅ addition increased, the ionic conduction increased up to 5 mol% V₂O₅ at which the highest conductivity was found to be $8.318 \cdot 10^{-2}$ Ω^{-1} cm^{-1} at 700°C and then decreased. It has been proposed that γ-Bi₂O₃ phase contains a large number of oxide anion vacancies and incorporated vanadium cations at tetrahedral sites which affect the oxygen sublattice of the crystal structure.

Introduction

Solid electrolytes are the most important components of solid state electrochemical devices, which are becoming increasingly important for applications in energy conversion, chemical processing, sensing and combustion control. In the past several years, Bi₂O₃ polymorphs based solid materials have been intensely investigated as catalysts, structural and electronic promoters of heterogeneous catalytic reactions, and oxide ion conducting solid electrolytes in electrochemical cells. The polymorphs of Bi₂O₃ are also used in oxygen sensor production and for this application, a relatively high ionic conductivity of the solid electrolyte is required for the device performance. ZrO₂ based high oxide ion conducting solid electrolytes have been studied and reviewed in the past. Many other investigations have been performed on other solid electrolytes as an alternative to ZrO₂, e.g., Bi₂O₃, SnO₂ [1–5].

Bismuth trioxide itself shows a polymorphism which is determined by the stability relationship of the four polymorphs using DTA/TG and high temperature X-ray

---

* Author for correspondence: E-mail: turkoglu@erciyes.edu.tr

diffraction, and reported in the earlier works on the subject [5–7]. The body centred cubic (*bcc*) γ-form, face centred cubic (*fcc*) δ-form, tetragonal β-form, and monoclinic α-form are the four polymorphs of the Bi_2O_3. One of the stable phases of pure Bi_2O_3 at low temperature is the α-Bi_2O_3 which is reported as monoclinic or pseudo-orthorhombic [5–8]. When α-Bi_2O_3 is heated to about 730°C, transition to the δ-Bi_2O_3 occurs. This high temperature δ-Bi_2O_3 phase (it is known as a fluorite structure related phase) is stable between 730°C and melting point 825°C. On the cooling of the δ-form, large thermal hysteresis effects are present and the δ-phase transforms to one of the two intermediate phases which are β-form (formed at 650°C) and γ-form (formed at 639°C). The metastable tetragonal β-phase is formed at 650°C on cooling from the melt or from the high temperature phase. The γ-phase which is known as Sillenite group of compounds can be obtained by controlled cooling of β-Bi_2O_3. Usually these metastable phases transform to the α-phase in the temperature range of 650–500°C [5–8]. The *bcc* γ-Bi_2O_3 phase can only be obtained as room temperature stable phase by addition of small amounts of other dopant oxides, i.e., Y_2O_3, MoO_3, CoO, Sb_2O_3, WO_3, SrO, CaO, La_2O_3 and Gd_2O_3 [9–18].

The *bcc* γ-phase is characterized in the I23 space group. This phase isomorphous with the *bcc* compound $Bi_{24}Si_2O_{40}$, where bismuth atoms occupy the silicon sites in the crystallographic structure. Other investigations indicated that the pure γ-Bi_2O_3 contains $Bi_{26}O_{39}$ in the cell with lattice parameters in the range of 10.10–10.27 Å. This indicates that γ-Bi_2O_3 has the largest unit cell parameter of the series of the reported Sillenite group compounds. The γ-Bi_2O_3 phase is also reported to be isomorphous with several other metal oxides giving the general formula $Bi_{24}M_2O_{39}$. It has not a perfect crystal system. On the other hand, the crystal lattice has the perfect structure where the *M* cation is tetravalent giving the general formula $Bi_{24}M_2O_{40}$ in the unit cell. For example, γ-form is isomorphous with $Bi_{24}^{3+}Bi^{5+}Fe^{3+}O_{40}$ and has the composition $Bi_{25}^{3+}Bi^{5+}O_{40}$, where the two tetrahedral sites are occupied by Bi^{3+} and Bi^{5+} ions. In addition to these, the structure of isomorphs which are $Bi_{12}GeO_{20}$, and $Bi_{38}ZnO_{60}$ have been determined. It has been proposed that pure γ-Bi_2O_3 contains $Bi_{26}O_{39}$ or $Bi_{26}O_{40}$ or $Bi_{24}O_{36}$ formulas in the unit cell. The Bi_2O_3 host lattice forms a cage type structure that can accommodate small metal ions in a tetrahedral coordination of oxygen atoms at the positions of (0,0,0) and (1/2,1/2,1/2). For stoichiometric compounds of this type, all particular cationic and anionic sites in the *bcc* unit cell are fully occupied. For non-stoichiometric compounds, metal ions are not quadrivalent so that the structure should contain fractionally occupied sites. In other words, γ-Bi_2O_3 has some vacancies in structure which can be described as the distorted defect crystal structure [6, 7, 18].

Several authors have tried to predict what kind of materials would have high oxide ion conductivity [9–15]. Often the structure of the materials is thought to be an important property when oxide ion conduction is considered. In many studies, the electrical conduction of the mixed oxides in the system of Bi_2O_3 –M_xO_y (*M*=Sb, Mo, Sr, La, Ca, W, Gd, Y, Ba, Pb, Si, Fe) have been investigated. To our knowledge of the related literature, all of the solid solution regions, and phases of this system have cubic crystal structure and they all show oxygen ionic conductivity [11, 12, 18]. These

materials are mainly the fluorite type solid solution regions based on the oxides tetravalent metals containing lower valence metallic oxides. Relatively large amounts of oxygen ion vacancies are present in the unit cell so that their conductivity is mainly ionic and O^{2-} ions are the mobile charge carries. Usually the higher temperatures and larger amounts of doped oxide materials cause increasing the oxygen ionic conductivity of the γ-Bi$_2$O$_3$ based solid solution [10–15, 18].

We have carried out this work in order to investigate the effect of V$_2$O$_5$ doping in Bi$_2$O$_3$. After accomplishing the stability of γ-Bi$_2$O$_3$ phase, we have examined electrical and thermal properties of this solid electrolyte. We have determined lattice parameters at room temperature for each doping ratio. The effects of temperature and doping ratio on the electrical properties were investigated and the obtained results were related and discussed.

Experimental details

The powder samples in our study were prepared by mixing the appropriate amount of monoclinic bismuth sesquioxide (99.99% Merck) and vanadium penta oxide (99.99% Merck) without further purification. The solid mixtures that contained different amounts of V$_2$O$_5$ doping (1 to 7 mol% V$_2$O$_5$) were prepared. Mixing and homogenizing were performed in an agate mortar. These oxide mixtures were calcined in a furnace, in gold crucibles, in air, at 650°C for 24 h. The calcined powders were ground and heat-treated at 700°C for 48 h. Calcined powders were re-ground and annealed at 750°C for 48 h. All these heat treatments were done as loose powders, in gold crucibles and in air. After the heat treatment procedure, loose powder samples were slowly cooled in the furnace by switching it off (uncontrolled). Each sample was separately ground into fine powder after the heat treatment. The color of the sintered specimens was observed to change from light yellow to dark yellow as the V$_2$O$_5$ content of the oxide mixture is increased. Some of these prepared powders were further heat treated separately at 700, 750 and 800°C in a vertical tube furnace in air and quenched in ice–water system. Quenching experiments were performed in order to clarify that phase transition to δ phase occurs at about 720°C.

Powder diffraction data of the samples were recorded with Bruker AXS D8 advanced diffractometer using a Bragg–Brentano geometry with graphite monochromator CuK$_\alpha$ radiation operated at 40 kV and 40 mA. Diffraction patterns were scanned by steps 0.002^o (2θ) over the angle range 10–90^o(2θ). Diffracted beams were counted with a NaI(Tl) scintillation detector and the obtained XRD patterns were compared with the reference data. Thermal measurements were made by using a simultaneous DTA/TG system (Shimadzu DT-40 type). The specimens, usually 11.4 mg in mass, were heated at a rate of 10°C min^{-1} from room temperature to 1000°C. Measurements were made in a dynamic air atmosphere using a platinum sample holder and α-Al$_2$O$_3$ inert reference substance.

Total conductivity (σ$_T$) measurements were made on samples pelletized at room temperature (diameter 10 mm, thickness ~1 mm) in a stainless holder ~1000 bar. Disk-shaped pellets were sintered for 24 h in air at 750°C. Scanning electron micros-

copy (SEM) revealed that the degree of compaction in all cases ranged between 80 and 95%. Silver electrodes were vacuum deposited as four narrow lines on one flat surface of the pelletized discs by dc sputtering technique. Fine silver wires were attached to the silver deposited regions using high conductivity silver paint. After making four point contacts on the pellet, it was heated in air at 400°C for half an hour to make the contacts stronger to handle and to reduce contact resistance. The heat treatment step at 400°C to dry the contacts was satisfactory for the purpose. At the same time this heat treatment did not cause any crystal structure change and no reaction between the sample and the contacts was observed. The ohmic character of the contacts was controlled by examining the I–V characteristics. The electrical conduction was measured in the temperature range 200–830°C by four probe arrangement (Keithley electrometer). The temperature of the samples during these measurements were determined by placing a thermocouple ~5 mm away from the sample. This thermocouple had a cold junction at 0°C. Temperature increments during these measurements were made smaller as the temperature approached to the phase transition temperature for this substance. The conductivity and temperature measurements of the samples at each temperature were made after thermal equilibrium was reached. We have made some rough calculations in order to determine the percentage of the oxygen ions lost due to direct current and concluded that it was quite insignificant (~1 part in 10^8).

Results and discussion

Samples of *bcc* γ-Bi$_2$O$_3$ were obtained by doping with V$_2$O$_5$ according to the formula of (Bi$_2$O$_3$)$_{1-x}$(V$_2$O$_5$)$_x$, x being 0.01≤x≤0.07. Mixed raw oxides mixtures were furnace cooled to room temperature after being annealed at 700 or 750°C. Heat treatment temperatures below 700°C did not produce γ-Bi$_2$O$_3$ phase. In this doping range, 1 to 7 mol%, all of the XRD patterns of the solid specimens were identified as having the body center cubic crystal symmetry and only peaks of γ-form were observed indicating single phase material. XRD patterns of 5 mol% V$_2$O$_5$ is given in Fig. 1. XRD patterns of other samples in this doping range were quite similar to the patterns given in this figure. Under the same heat treatment conditions, XRD measurements revealed that doping with more than 7 mol% V$_2$O$_5$ had caused the coexistence of γ- and δ-forms.

The relationship between the calculated unit cell parameters of γ-Bi$_2$O$_3$ and mol% V$_2$O$_5$ addition was illustrated in Fig. 2. As seen in this figure, lattice parameter decrease with increasing V$_2$O$_5$ substitution. This decrease in lattice parameters is sharp in 1–7 mol% doping range and it is much slower between 7 and 10 mol% addition; indicating a cross point at around 7 mol%. Furthermore, solid samples containing 8 to 10 mol% V$_2$O$_5$ have two phases coexisting. Peaks belonging to γ-phase had lower intensities from 8 to 10 mol% and their number is reduced. We therefore concluded that the solubility limit for V$_2$O$_5$ in *bcc* type (Bi$_2$O$_3$)$_{1-x}$(V$_2$O$_5$)$_x$ solid solution is ~7 mol% (x=0.07).

The decrease of lattice parameter with increasing V$_2$O$_5$ content is in good agreement with effective ionic radii considerations (reported ionic radii are 0.102 nm for Bi^{3+}, 0.075 nm for Bi^{5+}, 0.036 nm for V^{5+} and 0.074 nm for V^{3+} respectively [19]). Thus by increas-
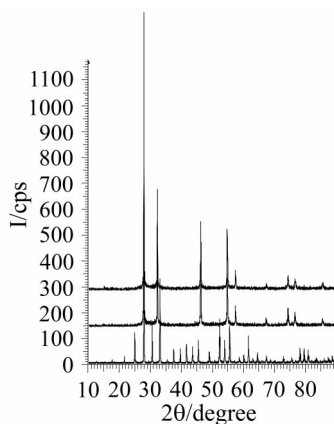
Fig. 1 XRD patterns of Bi_2O_3 doped with 5 mol% V_2O_5. At the top: *fcc* Bi_2O_3 (after quenching from 800°C). In the middle: *fcc* Bi_2O_3 (after quenching from 750°C). At the bottom: *bcc* Bi_2O_3 (after slow cooling from 750°C)
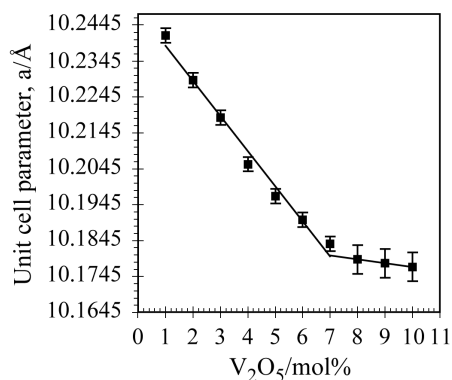

Fig. 2 The relationship between the amount of V_2O_5 addition and lattice constant of γ-Bi_2O_3 phase

ing the amount of V_2O_5, the crystal structure of the solid solution was modified toward smaller unit cell dimensions. On the other hand, phase formation of γ-Bi_2O_3 was very slow requiring a long heat treatment duration (at least 48 h). It was concluded from this fact that diffusion rate for vanadium ions into bismuth trioxide was quite low. Through this slow diffusion mechanism, vanadium cations preferentially substitute at the tetrahedral sites in the crystal structure, bringing one extra oxide ion with it. These oxygen anions are probably located randomly at the interstitial sites. When the charge balance is considered, incorporated vanadium cations would probably be trivalent and they locate at the tetrahedral sites. To accommodate incoming oxygen anions in the interstitial sites some bismuth cations (or vanadium cations) need to be pentavalent. In other words, as V_2O_5 addition increased, Bi^{3+} cations are spontaneously oxidized into pentavalent state. The structure now should have pentavalent bismuth ions and trivalent vanadium ions at the tetrahedral sites at an increasing rate with increasing V_2O_5 addition. Both Bi^{5+} ion and

Vanadium ions have smaller ionic radii than Bi^{3+} ions. This mechanism is considered to be responsible for reduction in lattice parameter with increasing doping ratio.

The color of the annealed samples follow a gradual change from light yellow (for x=0.01) to orange yellow (for x=0.07) and this color change is parallel to the increase in the value of x. The color change phenomenon may be considered to be related to the degree of nonstoichiometry. Increasing coloration in $(Bi_2O_3)_{1-x}(V_2O_5)_x$, series indicates an increasing nonstoichiometry with increasing addition ratio and as a result, samples should contain more defects at higher V$_2$O$_5$ levels. Oxygen nonstoichiometry in our samples is related with oxygen vacancies and interstitial oxygen ions. Since both type crystal defects contribute to electrical conductivity, we observed such a high conductivity in our samples.

The observed color change may be attributed to a charge transfer between the oxide ions and vacant d orbital of vanadium cations. Indeed, most of the metal oxides with high oxidation numbers are colored and these colors also stem from the charge transfer mechanism. Actually, the color of the untreated mixture of a certain x value differs remarkably from that of the treated samples. However, this difference is not surprising because the energy levels of the d orbital of the vanadium ions would change when introduced into the crystal structure of γ-Bi$_2$O$_3$ phase. The existence of O^{2-} vacancies in the crystal structure can also contribute to the color; because vacancy points (so-called 'color points') may be occupied by electrons through a light-absorption mechanism. Oxide-ion vacancies are also involved in the electrical conduction mechanisms and will be dealt with later in this paper.

Powder XRD patterns of the quenched samples (in Fig. 1 for 5 mol% V$_2$O$_5$ addition) were indexed to determine their crystal structure type for all doping ratios. On quenching from 700°C, the quenched samples remained in the same phase as prior to the final heat treatment and quenching, regardless of chemical composition. This showed us that heating to 700°C does not cause a phase transition which is also apparent in DTA/TG results. After quenched from 750°C, 1–7 mol% V$_2$O$_5$ added samples were in the δ-phase although they were γ-phase powders before this procedure. This finding indicates that heating to 750°C (above 720°C) causes a phase transition from γ-phase to δ-phase. 8, 9 and 10 mol% V$_2$O$_5$ doped samples contained both γ- and δ-phases before quenching and when quenched from 750°C they again contained γ- and δ-phases but they consisted of δ- and β-phases after they were quenched from 800°C. 1–7 mol% V$_2$O$_5$ doped powders were observed to be δ-phase after being quenched from 800°C similar to quenching from 750°C. These observations are in conformity with the following DTA/TG results.

DTA/TG diagram of 3 mol% V$_2$O$_5$ powder sample is seen in Fig. 3. According to the XRD and DTA/TG measurements, γ-form transforms into δ-form giving an endothermic peak at 720°C (T_{s_1} temperature). DTA/TG curve has a second endo effect at 832°C (T_{s_2} temperature) which was assigned to the melting point of formed δ-phase. TG curve reveals a very slow and gradual mass decrease in similarity with sublimation of Bi$_2$O$_3$ which is a well known phenomenon. The observed mass change in the TG curve at 965.2°C (T_{s_3}) corresponds to complete volatilization of the δ-Bi$_2$O$_3$. These DTA/TG analysis showed that the formed γ-Bi$_2$O$_3$ type solid solution is ther-
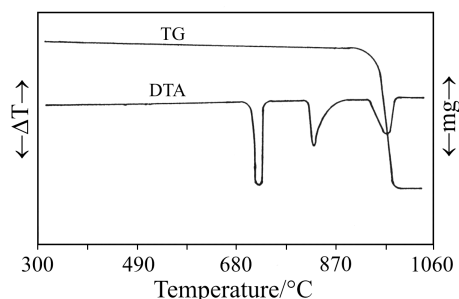
Fig. 3 Measured DTA/TG diagrams of γ-Bi$_2$O$_3$ phase doping with 3 mol% V$_2$O$_5$

mally stable between room temperature and 720°C. The observed T_{s_1}, T_{s_2} T_{s_3} and values for all addition ratios are given in Table 1.

Table 1 Observed DTA/TG values of γ-Bi$_2$O$_3$ solid solution doped with V$_2$O$_5$

V$_2$O$_5$ content/mol%	T_{s_1}/°C	T_{s_2}/°C	T_{s_3}/°C
1	719.8	830.3	963.5
2	720.1	831.0	964.4
3	720.0	832.1	965.2
4	721.5	832.3	965.1
5	722.2	832.5	964.8
6	722.5	832.0	965.1
7	723.0	833.2	965.5

T_{s_1} – Phase transition temperature of *bcc* Bi$_2$O$_3$
T_{s_2} – Melting points of *fcc* Bi$_2$O$_3$
T_{s_3} – Volatilisation temperature

In Fig. 4a, b, and c, typical Arrhenius plots of logσ_T –1/T for materials with 2, 5 and 7 mol% V$_2$O$_5$ contents are presented and σ_T plots for other samples are quite similar. These data were obtained during repeated heating runs at a constant heating rate in air. The electrical conductivity of γ-Bi$_2$O$_3$ doped with 1–7 mol% V$_2$O$_5$ increased with increasing temperature up to ~700°C. Beyond this temperature, conductivity sharply decreased up to about 720°C, then increased quickly up to ~820°C. A marked drop in total conductivity (between 700 and 720°C) was considered to be due to the phase transition from γ-Bi$_2$O$_3$ to δ-Bi$_2$O$_3$. In consistency with observation in conductivity, XRD and DTA/TG measurements also suggest that a polymorphic transition takes place, and the endothermic phase transition reaction was observed on the DTA curve at about the same temperature. The experimental results showed that δ-Bi$_2$O$_3$ exhibits higher conductivity than γ-Bi$_2$O$_3$ phase. This result is in agreement with the previous reports [9, 11]. We note that this behavior of the electrical conductivity can be described by simple Arrhenius equation, $\sigma_T = \sigma_0 \exp(-E_a/kT)$, where σ_T total electri-
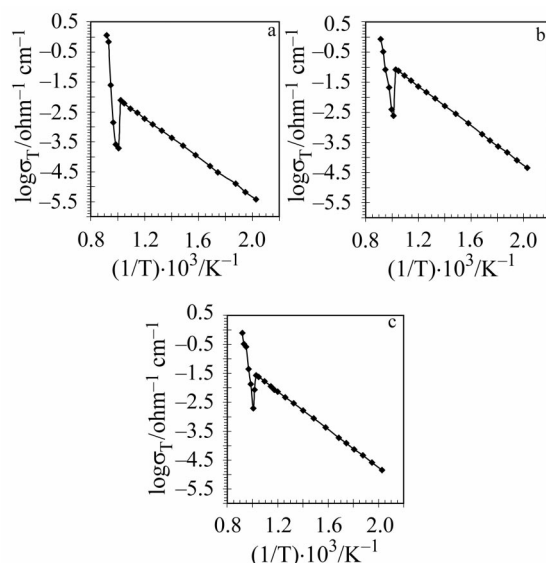
Fig. 4 The temperature dependence of total conductivity (σ$_T$) for γ-Bi$_2$O$_3$ phase;
a – 2 mol% V$_2$O$_5$ addition; b – 5 mol% V$_2$O$_5$ addition; c – 7 mol% V$_2$O$_5$ addition

cal conduction, σ$_0$ the preexponential factor, E_a activation energy, k Boltzmann constant, and T the absolute temperature.

The electrical conductivity in γ-Bi$_2$O$_3$ phase is mainly due to mobile oxygen ions as confirmed by other investigators [11, 17, 20–22]. This type of conductivity can be studied by measuring ionic transference numbers [12, 13]. This was not done quantitatively during this work, but we have carried out a qualitative experiment in order to show that the electrical conductivity in our samples is due to mobile oxygen ions. A thin 5% V$_2$O$_5$ doped bulk pellet with dimensions of ∅13×0.65 mm was subjected to an oxygen deficient atmosphere at one circular face and to an oxygen rich atmosphere at the other face. At 640°C, a DC potential difference of several mV was observed between the two faces, oxygen rich side being negatively charged. All necessary precautions were taken in order to make sure that the potential difference we observed was not of thermal origin. At the oxygen rich side of the sample, oxygen diffusion into the sample reached to equilibrium at a higher concentration of oxygen ion than the oxygen deficient side and as a result a potential difference was observed. This indicates that conductivity observed in our samples was mainly due to mobile oxygen ions.

The oxygen lattice points of the γ-phase should not completely occupied with oxygen ions. Oxygen vacancies are partly responsible for ionic conduction in our bulk samples. If the oxygen sublattice is fully occupied by O^{2-} ions, V$_2$O$_5$ doped γ-Bi$_2$O$_3$ phase would not show such an electrical conductivity. Some of the oxygen lattice points located around tetrahedral sites may be vacant forming an oxygen vacancy. These oxygen vacancies are filled with neighboring oxygen ions randomly at an increasing rate with increasing temperature. Jumping oxygen ions leave their for-

mer sites vacant thus another vacancy is formed; since this process is random, total oxygen flow is zero in any direction without an applied electric field.

As seen in Fig. 4, the conductivity of all samples increase with increasing temperature. It was proposed that this is connected with the ionic mobility which rises with the temperature. At elevated temperatures, thermal vibration energy of the ions increase causing higher oxygen ion jumping rate. Although oxygen vacancies are present in the crystal structure at low temperatures (below 200°C), thermal energy of the anions is not high enough for jumping out of their lowest energy positions. Thermal vibrations may also assist the jumping process momentarily by either shortening the jumping distance or by widening the jumping channels through the crystal.

Figure 5 shows the isotherms for σ_T vs. mol% V$_2$O$_5$. The electrical conductivity of V$_2$O$_5$ doped γ-Bi$_2$O$_3$ system increases systematically with increasing vanadium ion addition and reaches to a maximum for 5 mol% V$_2$O$_5$. For $x=0.05$ composition, the observed σ_T values are $3.574 \cdot 10^{-2}$ and $2.822 \cdot 10^{-3}$ Ω^{-1} cm^{-1} at 600 and 400°C respectively. Increasing conductivity with increasing addition is probably due to the intermediary role of interstitial oxygen ions. The observation that the ionic conductivity reaches to a maximum at about 5 mol% V$_2$O$_5$ content implies an optimum mobility for oxygen diffusion. Below this concentration, anionic mobility is increased with increasing interstitial oxygen ions and above this concentration, as the number of M^{5+} ions increase, oxygen ions are subjected to a stronger electrostatic attraction, making their mobility less probable. A decrease in conductivity then results for addition ratios higher than 5 mol%. Another possible mechanism for this maximum at $x=0.05$ may be gradual onset of the phase transition from γ-phase to $\delta+\gamma$ heterogeneous solid mixture, when addition ratio is further increased. Since $\delta+\gamma$ heterogeneous solid mixture is obtained for $x \geq 0.08$ compositions, a kind of loosening of the crystal structure toward a phase transition occurs for $x=0.06$ and $x=0.07$ samples. Increased background and decreased sharpness of XRD peak profiles support this effect. Decreasing conductivity for $x>0.05$ compositions may correspond to the conductivity decrease during phase transition on heating as seen on Fig. 4.
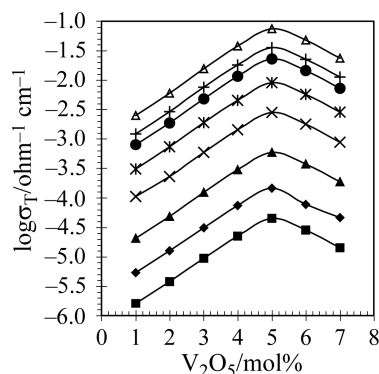

Fig. 5 Concentration dependence of the total conductivity of γ-Bi$_2$O$_3$ solid solution doped with V$_2$O$_5$; ■ – 220; ◆ – 260; ▲ – 320; × – 400; ∗ – 480; ● – 560; + – 600 and △ – 680°C

SEM (Scanning Electron Microscope) study revealed that grain size of the measured samples have a distribution in the range of 10 to 30 microns. There are some even smaller grains and fracture surface also have different shape grains. Grain boundaries are more significant for 1 and 2 mol% additions, and with increasing V$_2$O$_5$ addition, grains become better connected and larger. Especially 4 and 5 mol% V$_2$O$_5$ addition samples are better crystallized. Micro voids increases with increasing V$_2$O$_5$ addition.

Table 2 Activation energy (E_a) and exponential factor (σ_0) values of γ-Bi$_2$O$_3$ solid solution doped with V$_2$O$_5$

V$_2$O$_5$/mol%	E_a/eV (±0.001)	σ_0/Ω^{-1} cm^{-1} (±0.1%)
1	0.652	6.74
2	0.649	16.11
3	0.648	44.02
4	0.652	104.91
5	0.647	203.89
6	0.653	127.09
7	0.654	63.52

Calculated values of E_a and σ_0 as function of mol% addition are given in Table 2. As seen in table, activation energy value is almost constant. This may confirm the correlation of the constant values in E_a, which is a function of the electronic energy levels of the chemically interacting atoms in this type of solid phases. Constancy of E_a implies that crystallographic surroundings of the constituents of conduction, that are oxygen ions and vacancies, do not exhibit any appreciable change with increasing doping rate. Oxygen vacancies located around tetrahedral sites would either be in the center or in the corner. Nearest neighborhood distance is corner to center, jumping distance is being about $a/2\sqrt{3}$ which corresponds to 295.6 and 294.0 pm for x=0.01 and x=0.07, respectively. In reference 17, in Sb$_2$O$_3$ doped γ-Bi$_2$O$_3$ phase samples, calculated activation energy values do not change with Sb$_2$O$_3$ content similar to our study and is about 40% higher than that of our samples. At 500°C in the Bi$_2$O$_3$–Sb$_2$O$_3$ system the electrical conduction of 2.5 mol% Sb$_2$O$_3$ doped Bi$_2$O$_3$ *bcc* sample is $1.8 \cdot 10^{-3}$ Ω^{-1} cm^{-1}. In our study, at the same temperature and composition V$_2$O$_5$ doped sample was found to be $2.4 \cdot 10^{-3}$ Ω^{-1} cm^{-1}. This difference may originate from the differences in unit cell parameters and in electronic configuration of Sb and V cations.

On the other hand, conductivity is directly related to the number of charge carriers and diffusivity. In the solid electrolyte (Bi$_2$O$_3$)$_{1-x}$(V$_2$O$_5$)$_x$ system, σ_0 value increases with increasing doping in the $0.01 \leq x \leq 0.05$ composition range. As discussed earlier, number of pentavalent metal ions increases with increasing addition, this may lead to a higher number of oxide ions attacking to metal cations and consequently producing more vacancies. In other words, higher doping rates introduces more de-

fects into the structure and since the most predominant defect in these materials are oxygen vacancies, as a result oxygen vacancies are increased. Interstitial oxygen ions which are brought to the structure by vanadium cations may also contribute to the migration process via playing an intermediary role.

Since σ_0 value decreases for additions higher than 5 mol%, another mechanism should be responsible for this effect. As mentioned above, increased electrostatic attraction within the crystal may partly be responsible as well as loss of long range order in the grains prior to the phase transition from γ-phase to δ-phase. Additions more than 5 mol% may cause the amount of oxide anion vacancies to decrease through some of the interstitial oxide ions filling the present oxygen vacancies due to high interstitial oxygen ion concentration in the crystal structure. To elucidate this phenomenon beyond doubt would be possible if single crystals of this phase can be grown with dimensions large enough to handle and to work on.

Conclusions

γ-Bi$_2$O$_3$ can be obtained as room temperature stable phase by doping with V$_2$O$_5$ which is soluble up to ~7 mol%. This *bcc* type Bi$_2$O$_3$–V$_2$O$_5$ solid solution with distorted defective fluorite structure is stable up to around 720°C but transforms to *fcc* δ-Bi$_2$O$_3$ phase at higher temperatures. This δ-Bi$_2$O$_3$ phase is obtained as room temperature stable phase by either quenching or melting (above ~830°C) and cooling. If the sample is slowly cooled without melting, reverse transition takes place and γ-Bi$_2$O$_3$ phase re-appears. The electrical conduction in this system predominantly exhibits oxide ionic conductivity which is due to migration of oxygen ions through the crystal structure. Oxygen ionic conductivity increases with increasing V$_2$O$_5$ content, reaching a maximum value of $8.318 \cdot 10^{-2}\ \Omega^{-1}\ \mathrm{cm}^{-1}$ at 700°C for 5 mol%. The ionic conductivity of this binary system is 1 or 2 orders of magnitude higher than that of the most commonly used solid electrolytes. In addition, the results of DTA/TG, and XRD measurements are consistent with the results of the electrical conduction measurements.

* * *

References

1 N. Arora, G. Deo, I. E. Wachs and A. M. Hirt, J. Catal., 159 (1996) 1.
2 E. Kh. Shokr, M. M. Wakkad, H. A. Abd El-Ghanny and H. M. Ali, J. Phys. Chem. Solids., 61 (2000) 75.
3 D. Lybye, F. W. Poulsen and M. Mogensen, Solid State Ionics, 128 (2000) 91.
4 S. Bernik and B. Ai, 33rd Int. Cong. on Microelectronics, Devices and Materials, September 24–26 1997, Slovenia, 87.

　5　J. P. Goff, W. Hayes, S. Hulls, M. T. Hutchings and K. N. Clausen, Phys. Rev. B.,
　　　59 (1999) 14202.
　6　H. A. Harwig, Z. Anorg. Allg. Chem., 444 (1978) 151.
　7　J.W. Medernach and R. L. Snyder, J. Am. Ceram. Soc., 61 (1978) 494.
　8　O. Turkoglu, M. Soylak and N. Külcü, Kuw. J. Sci. Eng., 26 (1999) 289.
　9　H. T. Cahen, T. G. M. Van Den Belt, J. H. W. De Wit and G. H. J. Broers, Solid State Ionics,
　　　1 (1980) 411.
10　T. Takahashi, T. Esaka and H. Iwahara, J. Appl. Electrochem., 7 (1977) 31.
11　H. A. Harwig and A. G. Gerards, J. Solid State Chem., 26 (1978) 265.
12　T. Takahashi, H. Iwahara and Y. Nagai, J. Appl. Electrochem., 2 (1972) 97.
13　M. Miyayama, S. Katsuta, Y. Suenaga and H. Yanagida, J. Am. Ceram. Soc., 66 (1982) 585.
14　G. Chiodelli, A. Magistris, G. Spinolo, C. Tomasi, V. Antonucci and N. Giordano, Solid State
　　　Ionics, 74 (1994) 37.
15　T. Mori, T. Ikegamit, H. Yamamura and T. Atake, J. Therm. Anal. Cal., 57 (1999) 831.
16　O. Turkoglu and M. Soylak, Asian. J. Chem., 14 (2002) 1698.
17　O. Turkoglu, M. Soylak and I. Belenli, Bull. Mater. Sci., 25 (2002) 101.
18　M. Miyayama and H. Yanagida, J. Mater. Sci., 21 (1986) 1233.
19　A. R. West, Basic Solid State Chemistry, Wiley, Chichester 1988, pp. 64, 390.
20　K. Kakinuma, H. Yamamura and T. Atake, J. Therm. Anal. Cal., 69 (2002) 897.
21　H. Haneda, I. Sakaguchi, S. Hishita, T. Ishigaki and T. Mitsuhashi, J. Therm. Anal. Cal.,
　　　60 (2000) 675.
22　K. Kakinuma, H. Yamamura, H. Haneda and T. Atake, J. Therm. Anal. Cal., 57 (1999) 737.